Optimal Radio Frequency Power Distribution in a Linear Accelerator using Beam Energy Measurements

Author(s):
Rezaeizadeh, Amin; Kalt, Roger; Schilcher, Thomas; Smith, Roy

Publication date:
2016-04

Permanent link:
https://doi.org/10.3929/ethz-b-000111273

Originally published in:
IEEE Transactions on Nuclear Science 63(2), https://doi.org/10.1109/TNS.2015.2491639

Published: IEEE Trans. Nuclear Science, vol. 63, no. 2, pp. 777-782, 2016.

Optimal Radio Frequency Power Distribution in a Linear Accelerator using Beam Energy Measurements

Amin Rezaeizadeh, Roger Kalt, Thomas Schilcher and Roy S. Smith

***Abstract*—A linear accelerator including several radio frequency (RF) stations can be viewed as one virtual RF station with a certain RF voltage (in amplitude and phase). This paper proposes an optimization scheme that, for a specified total beam energy gain, determines the klystrons output powers as well as the modulators high voltages optimally. The algorithm employs the nonlinear static characteristics curves of klystrons to determine analytically the input RF amplitude of the drive chain. The proposed algorithm facilitates the klystron operating point setting with an automatic procedure for the desired energy gain of a linac.**

***Index Terms*—Linear accelerator, Free electron laser, Radio frequency control, Supervisory control, Beam-based feedback, Klystron, Convex optimization.**

I. Introduction

A linear accelerator (linac) is composed of a sequence of RF stations, delivering high power RF to the accelerating structures. If the power is generated by klystrons, finding the optimal operating points of the klystrons is a topic addressed in this paper. In order to enhance the stability of the klystron output RF amplitude as well as the efficiency, it is preferable to operate the klystron close to saturation. In this case, the input amplitude jitter has minimal influence on the output amplitude. The saturating (maximum) power of the klystron can be controlled by the modulator high voltage. Due to operation close to saturation, the AM-AM (output RF amplitude versus input RF amplitude) characteristic curves of the klystron are nonlinear. This nonlinearity makes it not so straightforward to inversely find the input RF amplitude and the high voltage of the modulator from a specified klystron output power. Figure 1 illustrates the klystron output power versus the klystron drive chain input RF amplitude and the voltage of the high voltage power supply (HVPS). The dashed line denotes the saturating powers for each high voltage. Two curves of constant power are plotted to show that for a specified output power, several choices of high voltage and input amplitude are possible. However, with a given headroom to the saturation, the operating point can be uniquely determined. This topic has been previously studied in [1] by introducing the concept of operating point determination (OPD). In this paper, we consider a sequence of klystrons in a linac , in which the operating points are optimally determined according to the desired total energy gain. We refer to this concept as beam-based multiple operating point determination (BM-OPD). In this scheme, an optimization procedure minimizes the high voltages of the modulators, while keeping the total beam energy constant. Since, according to experiments, the breakdown rate of the klystron has a direct relation to the high voltage level, the proposed optimization reduces the probability of breakdowns. The approach is based on a convex optimization [2] that uses the klystron AM-AM models as well as the energy gains of the RF stations. The method has been successfully tested at the SwissFEL injector test facility using three RF stations as a small scale prototype of a linac . The SwissFEL is being developed and constructed at the Paul Scherrer Institut [3]. The SwissFEL injector and the linac RF drives operate in a pulsed mode at rate of 100 Hz. There are 26 RF stations in the SwissFEL C-band linac . The experimental results show that if one of the stations fails to deliver the specified power, the optimization unit redistributes the high voltages over the other stations so the energy loss is compensated by increasing the power of the remaining klystrons.

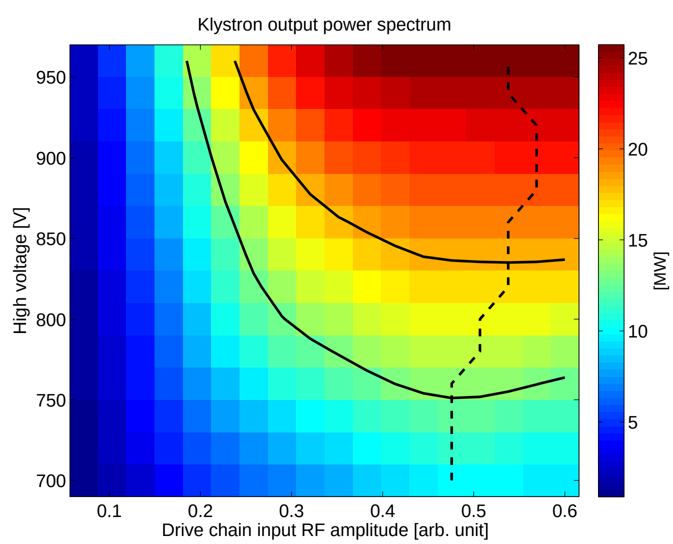

Fig. 1. The klystron output RF power versus the drive chain RF input amplitude and the modulator high voltage setting. The curves (solid line) show two examples of constant power contours. The dashed line indicates the saturating power. Any operating point on the right side of the dashed line should not be permitted as it drives the klystron into saturation.

Amin Rezaeizadeh is with Department of Electrical Engineering and Information Technology, ETH Zurich, CH-8092 Zurich, Switzerland, and also with the LLRF team at the Paul Scherrer Institut, AG-5232 PSI-Villigen, Switzerland (email: aminre@ee.ethz.ch).

Roger Kalt and Thomas Schilcher are with the Paul Scherrer Institut, AG-5232 PSI-Villigen, Switzerland.

Roy S. Smith is with Automatic Control Laboratory (IfA), ETH Zurich, CH-8092 Zurich, Switzerland.

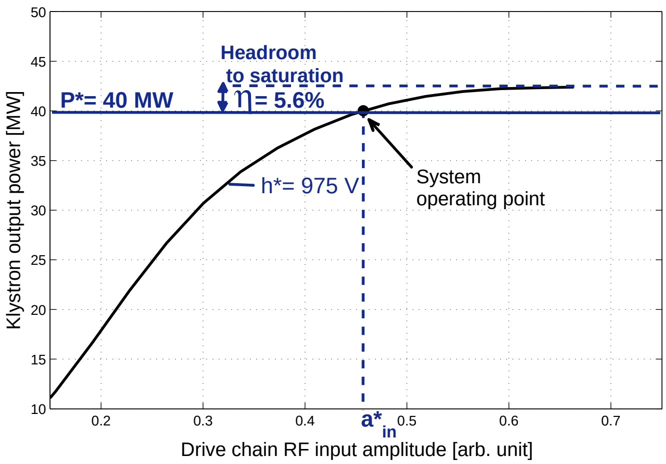

Fig. 2. The operating point definition of the klystron.

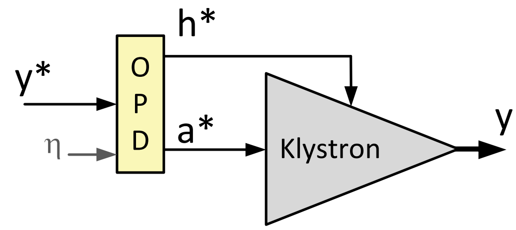

Fig. 3. The operating point determination (OPD) concept for the klystron. We denote by η the headroom to the saturation. The desired klystron output RF amplitude, y^*, and the headroom are the main inputs to the OPD. The corresponding high voltage, h^*, and the RF input amplitude, a^*_{in}, are analytically calculated through the OPD algorithm to generate the desired RF amplitude y at the klystron output.

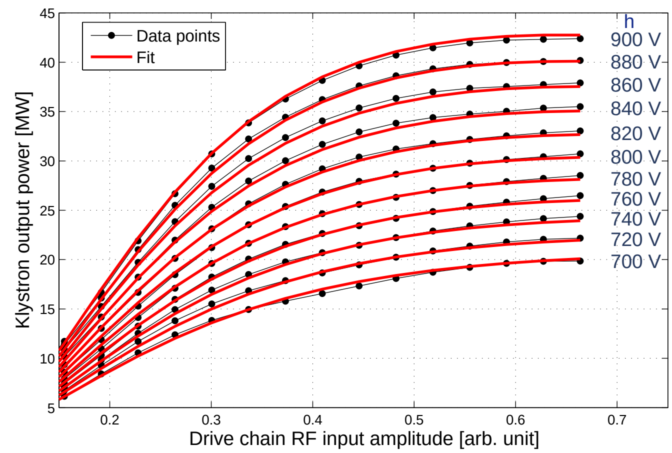

Fig. 4. The klystron output power, P, for different input amplitudes and high voltage power supply levels, h (numbers on the right side) of one RF station at the SwissFEL injector test facility. The models are depicted in thick solid lines.

This paper presents additional detail and materials and experimental results, not previously reported in [4]. In the following section, we briefly review the OPD functionality. Section III discusses the optimization scheme for determining the operating points of the klystrons. Section IV concludes the paper by giving the experimental results at the SwissFEL injector test facility.

II. Operating point determination

The klystron operating point is defined by the high voltage of the modulator, h^*, the output RF amplitude, y^*, and the drive chain RF input amplitude, a^*_{in} (see Fig. 2). We use the terms output amplitude and output power quite interchangeably, as one can be uniquely obtained from the other. The idea of determining the klystron operating point arises when one realizes that for a given output power, many choices of input amplitude and high voltage pairs are possible. However, as stated earlier, for the RF output amplitude repeatability, it is often required to operate the klystron close to saturation. The amount of headroom, from the operating point to the saturation level, is given in percent and is typically 1 to 5 $\%$. The headroom needs to be greater than a threshold which is defined as the difference of the saturation and maximum allowed output power. This is to give maneuverability to the amplitude controller when the RF amplitude feedback loop is closed.

With a given headroom to the saturating power, the klystron operating point can be uniquely determined. This implies that from all candidate operating points on the same contour, only one pair of high voltage and input amplitude satisfies the specified headroom. Finding this pair is the main function of the OPD. The OPD unit employs the klystron AM-AM characteristics models to analytically derive the corresponding high voltage and the input RF amplitude from a specified output RF amplitude of the klystron (see Fig. 3)[5], [6]. The details of the OPD are discussed in [1]. Typical klystron curves and the fitted models are shown in Fig. 4.

III. Optimization Scheme

In a linac with multiple RF stations, the total energy gain can be controlled via each individual klystron RF amplitude and the modulator high voltage. The way that the RF stations contribute to generate the desired total energy gain is the focus of this section. The distribution of RF power over the RF stations is done through an optimization problem. As a result, the required output RF power of each klystron is determined, which is then used by the OPD units to provide the required input amplitude as well as the modulator high voltage. Throughout this study, the headrooms, η, have predefined constant values. Moreover, we assume that the RF phases are set to zero, i.e. the “on-crest phase”.

In this section, we set up an optimization problem to reduce high voltages which have a direct relation to breakdown rate. Of course, the optimization problem is constrained to keep the total beam energy gain constant. We consider a linac including M RF stations. According to measurements, the relationship between the klystron maximum output amplitude and the high voltage is linear:

$$\frac{y_i}{1-\eta} = \gamma_i h_i + \xi_i, \tag{1}$$

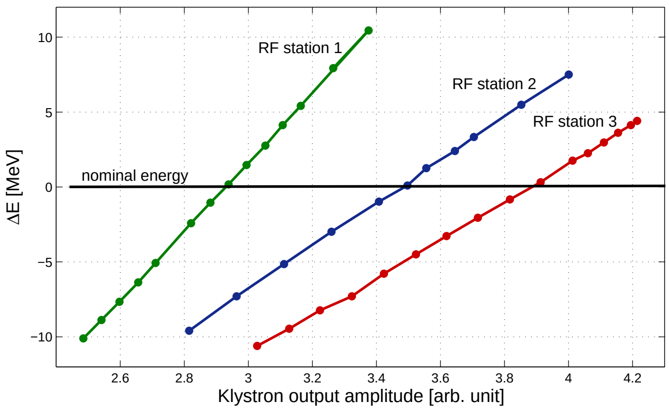

Fig. 5. Total beam energy scanning versus klystron output amplitude for different RF stations at the SwissFEL Injector Test Facility. The nominal energy, in this case, is 200 MeV.

where $\frac{y_i}{1-\eta}$ is the maximum output amplitude, with η representing the headroom. The h_i denotes the high voltage value of i-th klystron, and γ_i and ξ_i are constant parameters.

We denote by ΔE_{ref} to be the total desired energy deviation of M klystrons from the nominal energy. In other words,

$$\Delta E_{\text{ref}} := E_{\text{nom}} - E_{\text{ref}}, \tag{2}$$

where E_{nom} is the nominal energy, or the working point where the machine is calibrated, and where E_{ref} is the desired total energy setpoint asked by the user.

The running sum over all individual energy gain deviations should satisfy the desired reference energy, i.e.,

$$\sum_{i=1}^{M} \Delta E_i = \Delta E_{\text{ref}}. \tag{3}$$

On the other hand, the energy gain of each RF station, ΔE_i, is linearly related to the klystron output amplitude. That is,

$$\Delta E_i = \alpha_i y_i + \beta_i, \tag{4}$$

where y_i is the output amplitude of i-th klystron, and where β_i and α_i are constants. This can be also seen from the measurements results in Fig. 5 of the three RF stations at the SwissFEL injector test facility.

Substituting Eqs. (4) and (1) into (3), gives the following expression,

$$\sum_{i=1}^{M} \alpha_i(1-\eta)\gamma_i h_i = \Delta E_{\text{ref}} - \sum_{i=1}^{M} \left(\alpha_i(1-\eta)\xi_i + \beta_i\right). \tag{5}$$

We may take the cost function $J = \sum_1^M h_i^2$ as the risk function of breakdowns. This yields the following quadratic program:

$$\underset{h_i}{\text{minimize}} \ \sum_{i=1}^{M} h_i^2 \tag{6}$$

subject to

$$h_{i\text{min}} \le h_i \le h_{i\text{max}}, \quad i = 1, ..., M,$$

$$\sum_1^M \alpha_i(1-\eta)\gamma_i h_i = \Delta E_{ref} - \sum_1^M \left(\alpha_i(1-\eta)\xi_i + \beta_i\right),$$

where $h_{i\text{min}}$ and $h_{i\text{max}}$ are respectively the allowed lower and upper bounds on the high voltage of modulator i that can be set by the operator.

The optimization problem (6) lowers the high voltage values which consequently reduces the rate of breakdowns caused by large values of high voltages. It also reduces the total power consumption of the linac by minimizing the klystrons output powers. To be more precise, the optimal solution to (6) does not necessarily result in the minimum power consumption. In the klystron, the quantity $\kappa = \frac{I}{V^{1.5}}$ (I: klystron current, V: klystron voltage), known as the "perveance", is usually constant[7], [8], however, it can possibly change with the applied voltage. Therefore, to find the minimum power consumption, the cost function should be replaced by $\sum_1^M h^{2.5}$. For simplicity in analysis and to be able to use commercial optimization solvers, we consider the quadratic form.

IV. Experimental Results

Figure 6 illustrates the beam-based multiple OPD (BM-OPD) concept using three full-scale RF stations. The experiment parameters are given in Table I. We have $E_{\text{nom}} = 200$ MeV, $E_{\text{ref}} = 110$ MeV, and the headroom to the saturation is set to 5% for all klystrons. The control algorithm is implemented in Matlab scripts using CVX convex optimization solver [9], [10]. The communication to the machine is through EPICS process variables [11]. All stations' phases are scanned and set to the "on-crest" phase at the nominal energy of 200 MeV.

The optimization (6) is run for energy setpoints E_{ref}, and the actual measured beam energy is compared to the given setpoint. The results are plotted in Fig. 7. The error between the actual energy and the setpoint mainly comes from the model-system mismatch in both klystron modeling (OPDs) and the individual energy gain parameters. Nevertheless, this open-loop error can be corrected by introducing an "offset-free" property to the optimization problem (6). That is, the optimization is run for several iterations with the energy setpoint being updated according to

$$\Delta E_{\text{ref}}^{k+1} = \Delta E_{\text{ref}}^{k} + G\ e^k, \tag{7}$$

where superscript k denotes the time sample, G is a constant gain, and e^k is the measured energy error defined as

$$e^k := E_{\text{meas.}}^k - E_{\text{ref}}, \tag{8}$$

with $E_{\text{meas.}}^k$ denoting the measured energy [12].

The beam energy is measured at the end of the machine through the spectrometer camera (see Fig. 8). The position

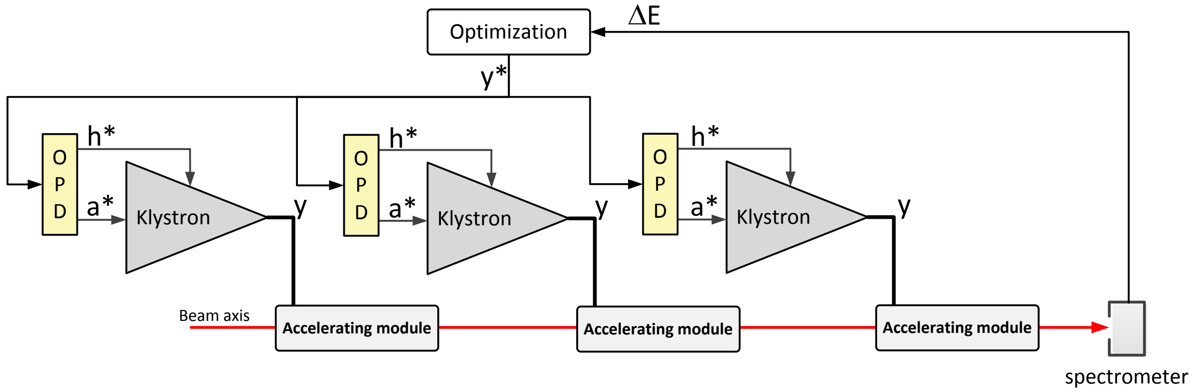

Fig. 6. The simplified schematic of the beam-based power distribution at the SwissFEL test facility. The beam energy is measured through the spectrometer camera and compared to the reference energy. The error is then used in the optimization unit to recalculate the klystrons' operating points. The optimal RF input amplitudes are determined through the OPD units. The headroom is set to 5% for all klystrons.

TABLE I
EXPERIMENT PARAMETERS

Parameter	Value
E_{nom}	200 MeV
E_{ref}	110 MeV
M	3
η	5%
G	0.5

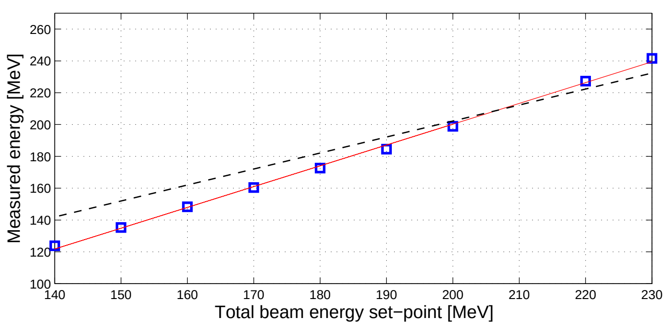

Fig. 7. The measured beam energy, $E_{\text{meas.}}$, versus the reference energy, E_{ref} (in solid line). The dashed-line represents the ideal open-loop response.

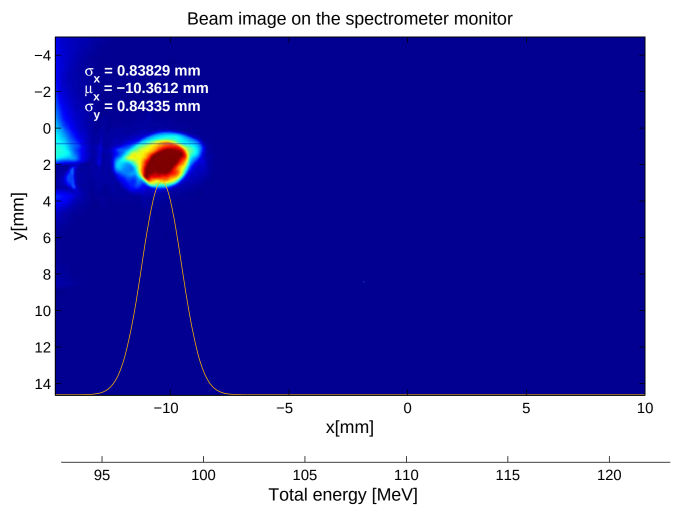

Fig. 8. The electron beam image at the spectrometer camera. The x-position of the beam gives an estimation of the beam energy. In this particular experiment, the image center, i.e. $x = 0$, corresponds to $E_{\text{ref}} = 110$ MeV. The beam energy in the current snapshot is 98 MeV.

of the beam spot on the x-axis gives a measurement of the energy.

A. Disturbance Rejection Scenario

In the following experiment, we study behavior of the BM-OPD under disturbance situation, particularly, a breakdown in one RF station. In this case, the disturbed RF station fails to deliver the required power and therefore the BM-OPD unit should be notified, for example through the Machine Protection System. The optimization is repeated with the following modified constraints on the disturbed station parameters h_j and α_j,

$$h_{j_{\min}} = h_{j_{\max}} = 0, \qquad \alpha_j = 0, \tag{9}$$

where subscript j represents the failed klystron.

Figure 9 illustrates the beam position on the spectrometer monitor with the disturbance occurring at time k=20. Figure 10 plots the high voltage power supply values of the three klystrons. The energy setpoint is $E_{\text{ref}} = 110$ MeV, and the high voltage values and input RF amplitudes are set according to the optimization in (6). After applying the settings, the measured beam energy is initially below the setpoint, as shown previously in Fig. 7. Closing a feedback loop around the measured beam position, according to Eq. 7, iteratively corrects the systematic error caused by model-system mismatch (see Fig. 9 from time k=0 to k=20). During this time, the high voltages values may change very slightly, although the changes are not distinguishable in Fig. 10.

At time $k = 20$, one RF station is set to off to perform the disturbance rejection test. Consequently, the beam disappears from the spectrometer monitor. As stated earlier, the BM-OPD repeats the optimization with modified constraints on the disturbed station and updates the high voltage values. After applying the updated RF settings, the beam appears on the

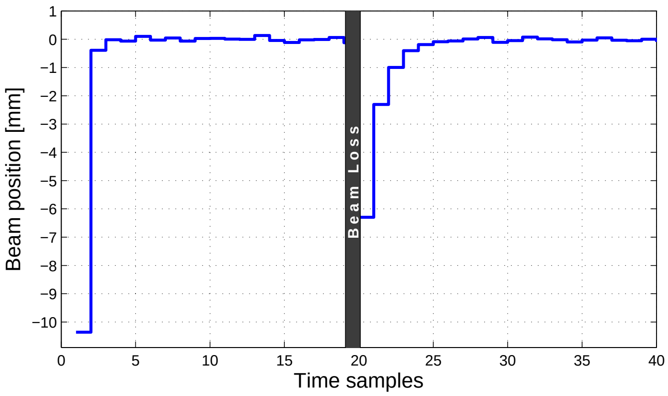

Fig. 9. The beam position measured on the spectrometer. The desired energy which, in this case, is 110 MeV, corresponds to zero position.

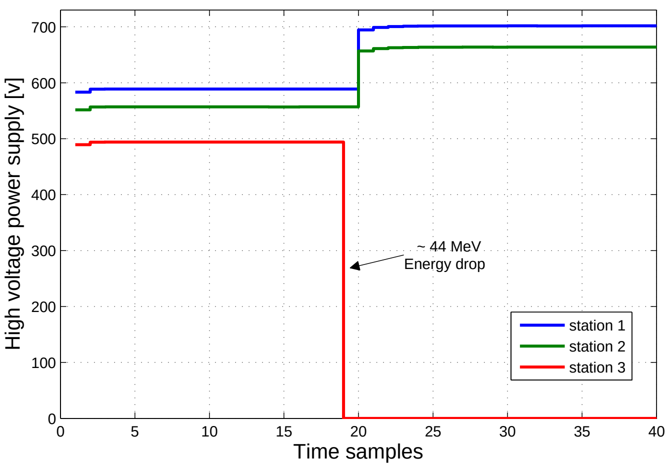

Fig. 10. The high voltage values of the three klystrons at the SwissFEL injector test facility. At time sample $k = 20$, one station is set to off to observe the disturbance rejection behavior of the BM-OPD. The remaining stations increase their power to compensate for the energy loss.

spectrometer, however, with slightly lower energy than the setpoint. The error is iteratively corrected and the beam spot is finally brought to the center at the energy of 110 MeV. As we can see from Fig. 10, the two remaining stations increase their high voltages to compensate for the energy loss. The drive chain RF input amplitudes are plotted in Fig. 11. According to the klystrons characteristics curves, the input RF amplitude corresponding to the saturating output power is inversely related to the high voltage of the modulator. Therefore, as the high voltage increases, the input RF amplitude is decreased to keep the same headroom.

During the whole time horizon $0 < k < 40$, the optimization runs for every time sample. The beam recovery time depends mainly on how fast the high voltage modulators can react to the setpoint changes. In this experiment, the beam is recovered and brought to the desired energy within a minute from the disturbance.

V. Conclusion

An automatic procedure is developed to optimally set the RF input amplitude and modulator high voltage of multiple

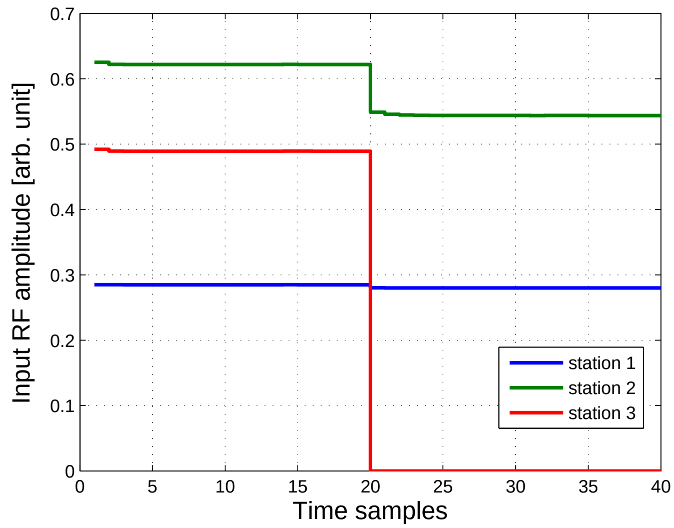

Fig. 11. The input RF amplitude to the klystron drive chain.

klystrons in a linac . The approach is based a convex optimization with constraints on the total energy gain of the linac as well as the high voltage bounds. The main objective of the proposed method is to determine the operating points of klystrons according to the specified total energy gain. Experiments show that the station breakdown rate increases significantly as the high voltage increases. Therefore, the optimization proposed here minimizes the sum of squared high voltages of the modulators which in turn lowers the breakdown rate of the machine as well as the total power consumption. The control scheme operates in an iterative manner, meaning that beam measurements are used to update the RF parameters. The optimization performs continuously until the user-specified energy gain is met. The experimental results at the SwissFEL injector test facility demonstrate that the desired beam energy gain can be achieved within 15% error in one run of the algorithm. This error can be corrected as the procedure is repeated iteratively in a slow rate (nearly 1 Hz). The algorithm is also tested for disturbance rejection experiment in which one RF station fails to generate the specified power. In the disturbance rejection scenario, if enough reserve power is available, the remaining stations contribute to compensate for the energy loss. The main objective of the BM-OPD is to bring the machine close to the desired operating point (in terms of energy gain). This optimization should be run after beam phasing, i.e. after finding the “on-crest” phases. Once the high voltage values are set, for fast and precise control of the beam energy, the pulse-to-pulse RF and possibly beam-based feedback loops must be closed.

Acknowledgment

The authors would like to thank Thomas Schietinger, the beam time coordinator of the SwissFEL injector test facility, and also the LLRF and the RF team who made this research possible.

REFERENCES

[1] A. Rezaeizadeh et al., "Model-based klystron linearization in the SwissFEL test facility", *Proceedings of the 36th International Free Electron Laser Conference*, Basel, Switzerland, August 2014.

[2] S. Boyd and L. Vandenberghe, *Convex Optimization* , Cambridge University Press, 2004. Retrieved October 15, 2011.

[3] Romain Ganter et al., SwissFEL Conceptual Design Report, Technical Report PSI Bericht Nr. 10-04, Paul Scherrer Institut, Villigen, Switzerland, 2010.

[4] A. Rezaeizadeh et al., "Beam-based power distribution over multiple klystrons in a Linear accelerator", *Proceedings of the 6th International Particle Accelerator Conference*, Richmond VA, USA, 2015.

[5] Ch. Rapp, "Effects of HPA-Nonlinearity on a 4-DPSK/OFDM-Signal for a Digital Sound Broadcasting System", *Proc. of 2nd European Conference on Satellite Communications*, Liege, Belgium., Oct. 1991, pp. 179184.

[6] A. J. Cann, "Non-linearity Model With Variable Knee Sharpness", *IEEE Trans. Aerosp. Electron. Syst.* vol. 16, no. 6, pp. 874877, Nov. 1980.

[7] S. Simrock and Z. Geng, "Klystron", 4th Linear Collider School, Beijing, China, 2009, LLRF and HPRF.

[8] A.W. Chao and M. Tigner, *Handbook of Accelerator Physics and Engineering*, World Scientific, 1999, p. 100.

[9] Michael Grant and Stephen Boyd. CVX: Matlab software for disciplined convex programming, version 2.0 beta:
http://cvxr.com/cvx.

[10] Michael Grant and Stephen Boyd. Graph implementations for nonsmooth convex programs, Recent Advances in Learning and Control, V. Blondel, S. Boyd, and H. Kimura, editors, pages 95-110, Lecture Notes in Control and Information Sciences, Springer, 2008:
http://stanford.edu/~boyd/graph_dcp.html.

[11] Experimental Physics and Industrial Control System (2015):
http://www.aps.anl.gov/epics

[12] G.F. Franklin et al., *Digital Control of Dynamic Systems*, Addison Wesley, 1998.